ORGANIC CHEMISTRY FRONTIERS

CCS 中国化学会 CHINESE CHEMICAL SOCIETY

SIOC

ROYAL SOCIETY OF CHEMISTRY

Angular ladder-type meta-phenylenes: synthesis and electronic structural analysis

Journal:	*Organic Chemistry Frontiers*
Manuscript ID	QO-RES-08-2020-000924.R1
Article Type:	Research Article
Date Submitted by the Author:	13-Sep-2020
Complete List of Authors:	boddeda, anitha; Marquette University, Chemistry Hossain, Mohammad Mosharraf; Miami University, Chemistry Mirzaei, Mohammad Saeed; Razi University, Chemistry Lindeman, Sergey; Marquette University, Department of Chemistry Mirzaei, Saber; University of Pittsburgh, Chemistry Rathore, Rajendra; Marquette University, Department of Chemistry

ARTICLE

Angular ladder-type *meta*-phenylenes: synthesis and electronic structural analysis

Received 00th January 20xx,
Accepted 00th January 20xx

DOI: 10.1039/x0xx00000x

Anitha Boddeda,[a] Mohammad Mosharraf Hossain,*[§a] M. Saeed Mirzaei,[b] Sergey V. Lindeman,[a] Saber Mirzaei*[c] and Rajendra Rathore[‡a]

Herein, we report the synthesis of two new series of angular (all-syn) ladder-type *meta*-[n]phenylenes (LMP, n = 3-8). One series contains keto groups at the termini bridges, denoted angular keto (AKn), the second contains alkyl groups at all bridge sp^3 carbons, denoted angular alkyl (AAn). Their electronic and structural properties were delineated by a combination of electrochemistry and spectroscopic (UV-Vis and emission) methods and further supported by DFT calculations. Interestingly, experimental and DFT data show that changing the bridging group at the termini from alkyl (AAn) to keto (AKn) gives an increase in the first reduction potentials and LUMO energies, as the π-system is extended. Also, the charge (de)localization behavior is different for these two species; while the AAn compounds stablize charge with Robin-Day class III, the AKn compounds show a clear switch from class III to class II. In comparison with the linear analogues (LKn and LAn), DFT results reveal a shape independency of the charge (de)localization mechanism in acceptor-π-acceptor series (AKn/LKn).

Introduction

Over the past few decades, significant strides have been taken toward the design of polycyclic aromatic hydrocarbons (PAHs) that offer a vast diversity of topologies along with unique and improved photoluminescence features, electrochemical/thermal stability, and effective charge transport.[1-8] Among PAH compounds, the synthesis of ladder-type poly-phenylenes (LPP)[9] has been a topic of ever-growing interest mainly due to their conjugated, flat and conformationally rigid structures, which promise broad applications in electronic devices.[4, 10-15]

The connectivity of phenylene moieties (*meta* or *para*) and position of the bridged sp^3 carbons (*syn* or *anti)* are the source of structural diversity in LPPs (Chart 1). To date, most efforts have been devoted to the development of the linear *para* isomer and its derivatives (Chart 1). Other configurations like bent-shaped *meta*-phenylenes (LMPs) remain mostly unexplored,[16, 17] as these cross-conjugated[18] LPPs suffer from poor effective global conjugation[19, 20] which has been attributed to the anti-resonance and destructive quantum interference (QI) phenomena.[21-24] It should be noted that the incorporation of *meta*-phenylene into the *para*-phenylenes in an alternating fashion follow the same trend and allow for a significant portion of cross-conjugation which has been observed and justified both experimentally and computationally.[25-27] Despite the acceptance of this behavior, Ratner revealed that cross-conjugated molecules, like polyenes, can show exceptional behavior in electron transmission.[28, 29]

In addition to the overall architecture of LPPs, substituents have large effects on their electronic properties and applications. For instance, several applications of both electron-rich (e.g. polyfluorenes)[4, 30] and electron-deficient (electron transporting) systems are well-established in

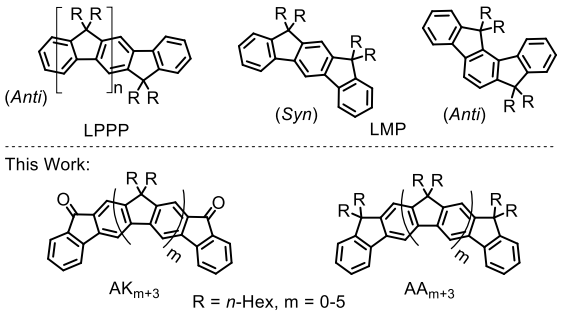

Chart 1. The general structure of *anti*-ladder-type *para*-polyphenylene (LPPP), *syn*- and *anti*-ladder-type *meta*-phynylene (LMP) and all-*syn* LMPs in this work.

[a] *Department of Chemistry, Marquette University, Milwaukee, WI 53201-1414, United States. E-mail: hossaimm@miamioh.edu*
[b] *Department of Organic Chemistry, Faculty of Chemistry, Razi University, Kermanshah, Iran.*
[c] *Department of Chemistry, University of Pittsburgh, Pittsburgh, PA 15260, United States. E-mail: saber.mirzaei@pitt.edu*
§ Present Address: Miami University, Department of Chemistry & Biochemistry, Oxford, Ohio 45056, United States.
‡ Deceased February 16, 2018.

Electronic Supplementary Information (ESI) available: containing Procedures for the synthesis of AKn and AAn compounds; $^1H/^{13}C$ NMR spectra of AKn and AAn and all intermediate molecules; crystal structures (CCDC numbers 1998629-1998633), computational details. See DOI: 10.1039/x0xx00000x

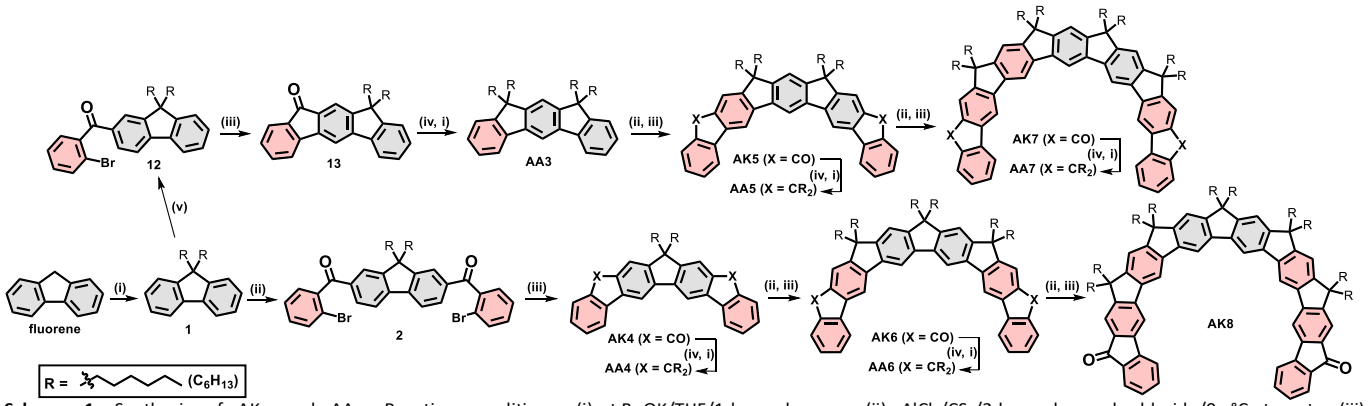

Scheme 1. Synthesis of AKn and AAn; Reaction conditions: (i) *t*-BuOK/THF/1-bromohexane; (ii) $AlCl_3/CS_2$/2-bromobenzoyl chloride/0 °C to r.t.; (iii) $Pd(OAc)_2/PCy_3{\cdot}HBF_4/K_2CO_3$/DMA; (iv) Pd/C (10%)/$H_2$/EtOAc/$HClO_4$; (v) $AlCl_3/CH_2Cl_2$/2-bromobenzoyl chloride/0 °C to rt.

different fields such as organic light-emitting diodes (OLEDs).[31] One of the determining factors toward an efficient electron-transporting material[32-34] is its high electron affinity (low-lying LUMO) which can be achieved by incorporation of electron-withdrawing substituents.[35] Thus, the good performance of fluorenone as electron deficient unit has been acknowledged in the literature.[36-38] It should be noted that the incorporation of electron withdrawing groups are mainly done through the synthesis of electron donor and acceptor groups bridged by a π linkers (donor-π-acceptor, D-π-A),[39, 40] rather than donor-π-donor (D-π-D) and acceptor-π-acceptor (A-π-A) systems.[41]

In this study, we report the synthesis of a series of angular (all-*syn*) ladder-type *meta*[*n*]phenylenes (LMPs). We aim to: (i) develop a new synthetic approach for diversifying LPPs, (ii) investigate structure-property relationships via comparison with their linear counterparts, and (iii) evaluate conjugation length effects on the A-π-A species. We prepared compounds with two different termini: angular keto-bridged (AKn) and angular alkyl-bridged (AAn, Chart 1). The structural and electrochemical properties of the synthesized molecules were determined experimentally and predicted using density functional theory (DFT) methods. Moreover, we compared their electronic and structural features to their linear isomers, linear ketos (LKn) and linear alkyls (LAn), using DFT methods. The results revealed an increasing evolution in the first reduction potentials and LUMO energies of AKn when the π-system is extended. This indicates the diminution of the charge delocalization in the A-π-A series. The details of these findings are discussed herein.

Synthesis. The 9,9-dihexylfluorene (**1**) was prepared on gram scale with the reaction of fluorene with 1-bromohexane in tetrahydrofuran (THF) using *t*-BuOk as the base (Scheme 1). The subsequent diacylated product (**2**) is obtained in excellent yield by treating **1** with two equivalents of 2-bromobenzoyl chloride and four equivalents of $AlCl_3$ in CS_2. For the cyclization reactions, we employed the palladium(II) acetate ($Pd(OAc)_2$) as the catalyst and tricyclohexylphosphinetetraflouroboric acid ($PCy_3{\cdot}HBF_4$) as the ligand.[42] The reaction mixture was heated in *N,N*-dimethylacetamide (DMA) to obtain the first even LMP (**AK4**). The synthesis of **AA4** compound was accomplished by reducing the **AK4** and alkylating following the same approach as for the synthesis of

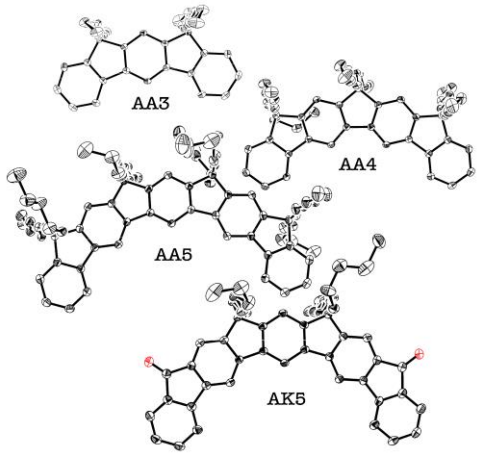

Fig. 1 Crystal structures (obtained at 100 K) of AA3, AA4, AK5 and AA5 molecules; hydrogen atoms and solvent molecules are deleted for clarity; thermal ellipsoids are set at 50% probability level; the C and O atoms are colored grey and red, respectively.

1. The AK6 and AK8 molecules were obtained using similar sequence as used for AK4. For the synthesis of odd-membered compounds we reacted the **1** with one equivalent of 2-bromobenzoyl chloride in CH_2Cl_2 as the solvent to obtain the molecule **12** as an important precursor for the subsequent compounds. It should be noted that the **AK3** molecule prepared following the procedure reported by Wei et al.[43]

The structures of all AKn and AAn compounds and the intermediate species were characterized by $^1H/^{13}C$ NMR and mass spectrometry (see the electronic supplementary information for experimental details). Crystal structures were obtained for **AA3**, **AA4**, **AA5** and **AK5** (Fig. 1), which showed the expected angular and flat geometry. In addition, we were able to obtain the single crystal structures of the precursor of **AK6** compound (Fig. S12, ESI).

Continuation of adding more phenylenes leads to the synthesis of *m*-phenylene macrocycle (i.e. closed form with 10 phenyl units, AA10); however, we have not been able to accomplish that synthesis. The similar cyclic oligomers with 8 and 10 phenylene units were synthesized by Wu and coworkers which showed bowl-shaped and planar geometry, respectively.[44]

Table 1. Experimental and DFT calculated values of the first redox potential (E_{red1}/E_{ox1}, V vs. SCE), maximum absorption and emission (λ_{max}, nm), energy of LUMO and HOMO (eV) and optical band gap (E_g, eV).

	E_{red1}[a]	absorption[b]	emission	E_{LUMO}[c]	E_g[d]		E_{ox1}[a]	absorption[b]	Emission	E_{HOMO}[c]	E_g[d]
AK3	-0.98(-0.97)	329(311)	530	-3.42(-2.38)	3.63(4.28)	AA3	1.43(1.44)	339 (298)	342	-5.83(-6.01)	3.58(5.50)
AK4	-1.18(-1.21)	434(430)	487	-3.22(-2.21)	2.57(4.13)	AA4	1.30(1.28)	352 (311)	357	-5.70(-5.86)	3.43(5.28)
AK5	-1.35(-1.35)	419(419)	506	-3.05(-1.94)	2.58(4.19)	AA5	1.23(1.22)	360 (318)	365	-5.63(-5.77)	3.37(5.16)
AK6	-1.35(-1.36)	422(421)	513	-3.05(-1.92)	2.56(4.06)	AA6	1.18(1.20)	364 (322)	369	-5.58(-5.72)	3.33(5.09)
AK7	-1.36(-1.37)	430(421)	513	-3.04(-1.90)	2.56(3.96)	AA7	1.17(1.17)	367 (325)	371	-5.57(-5.69)	3.32(5.05)
AK8	-1.38(-1.37)	430(421)	516	-3.02(-1.90)	2.54(3.90)	AA8	---(1.17)	--- (327)	---	---(-5.67)	---(5.02)

In parentheses are: [a] DFT values of first redox potential (E_{red1}/E_{ox1}, scaled to experimental data); [b] DFT maximum absorption (λ_{max} nm); [c] DFT energy of LUMO/HOMO (eV) and [d] DFT E_g ($E_{LUMO-EHOMO}$, eV); all DFT values are reported at BLYP35/6-31+G(d,p)+SMD(CH_2Cl_2) level of theory.

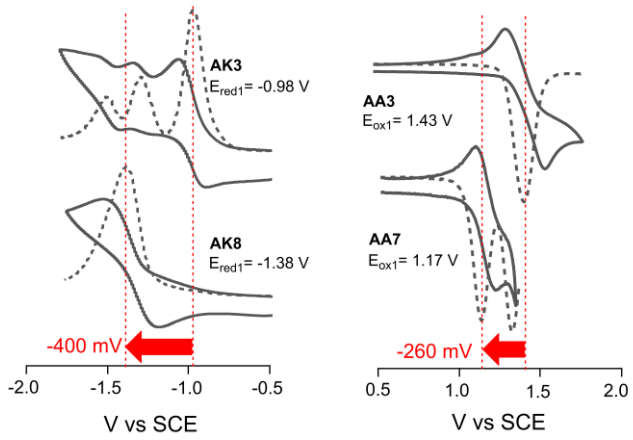

Fig. 2 Cyclic (—) and square-wave (...) voltammograms of AK3 and AK8 (left, in 1:1 MeCN:C_6H_6) and AA3 and AA7 (right, in CH_2Cl_2) compounds at a scan rate of 100 mV s^{-1} and 22 °C; The CV and SW of other species are provided in the ESI.

They used hydrogen on the bridged sp^3 carbons which allowed them to do the oxidative dehydrogenation reaction in the last step to obtain the interesting totally conjugated structures with unusual global aromaticity.[44, 45]

Spectroscopy. The redox features of all AKn and AAn were collected by subjecting them to electrochemical reduction/oxidation at a platinum electrode as a 2 × 10^{-3} M solution containing 0.1 M tetra-butylammonium hexafluorophosphate (*n*-Bu_4NPF_6) as the supporting electrolyte. The cyclic voltammograms of all species showed reversible waves for the first reduction (AKn) and oxidation (AAn) processes (Fig. S3, ESI).

As depicted in the Fig. 2, The E_{red1} is -0.98 V and -1.38 V for **AK3** and **AK8**, respectively. These values indicate a significant increase (~400 mV) in the E_{red1}. Comparing the E_{red1} for all AKn species (Table 1) shows that the E_{red1} moves toward more negative values with increasing number of phenylene units. However, this change is more drastic when moving from **AK3** to **AK5** and converges for the rest (Table 1). These data show that for the studied A-π-A systems in this paper, extending the conjugation decreases the interaction between the ends and increases the LUMO level. It should be noted that the increasing trend of the LUMO level with extending the π system is observed before for different compounds. For example, the experimental data (electron affinities) for benzo-, naphtho-, and anthraquinones showed that the expansion of the π system reduces the electron affinity.[46] Moreover, this effect, increasing the LUMO energy by increasing the π system, has also been observed in the solution phase (CV studies) when electron withdrawing groups like nitro are attached to the larger aromatic system.[47, 48] In addition, recently, our group investigated the end cap substitution effects on poly-*para*-phenylenes wherein experimental and DFT results confirmed that the electron rich groups (alkoxy and alkylamine) reverse the evolution of HOMO energies with respect to the number of phenylene units and in turn reverse the expected oxidation potentials.[41, 49]

On the other hand, the first oxidation potential (E_{ox1}) of AAn compounds decreases with an increase in length, as expected. The E_{ox1} is ~1.43 V and ~1.17 V for **AA3** and **AA7**, respectively (Table 1 and Fig. 2), in accordance with an increase in HOMO energy with respect to length. Having these data, we calculated the LUMO and HOMO energies for AKn and AAn molecules respectively (Table 1) by employing $E_{1/2}$ of the first redox event according to $E_{HOMO/LUMO} = -[E_{1/2} + 4.4]$ eV.[50, 51]

To explore the frontier molecular orbitals (FMOs) of our molecules, we collected the absorption and emission spectra of both AAn and AKn compounds (Table 1 and Fig. 3 and 4). As listed in Table 1, the absorption maxima for **AA3-AA7** clearly show a bathochromic shift from **AA3** (339 nm) to **AA7** (367 nm). The same trend is observed for the emission bands, which is a common optical behavior of conjugated systems.[52] However, cross conjugation causes very little shift in optical spectra.[53-55]

Comparing the AAn with AKn reveals that the AKn series does not show any correlation with increasing number of phenylenes; however, show us the red shift of both absorption (except the **AK3**) and emission spectra by changing the termini bridges from alkyl to keto. Interestingly, this changing leads to huge difference between the Stokes shift values. While the AAn compounds indicated very small value (~341 cm^{-1}), the AKn species showed much higher average value (~6016 cm^{-1}, Table 1 and Fig. 3 and 4). These larger values of AKn series can be useful in the optical materials as they benefit from lower self-quenching.[56-58]

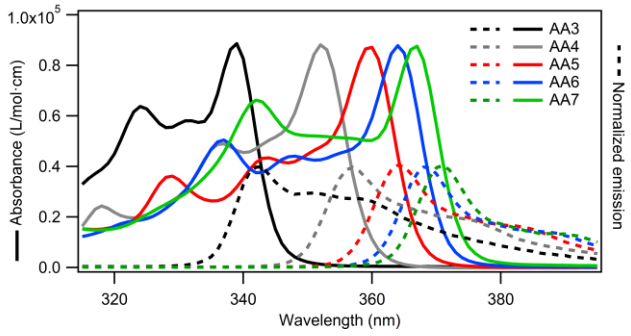

Fig. 3 Compilation of the absorption (—) and emission (...) spectra of the AA3-AA7 (in CH_2Cl_2) at 22 °C.

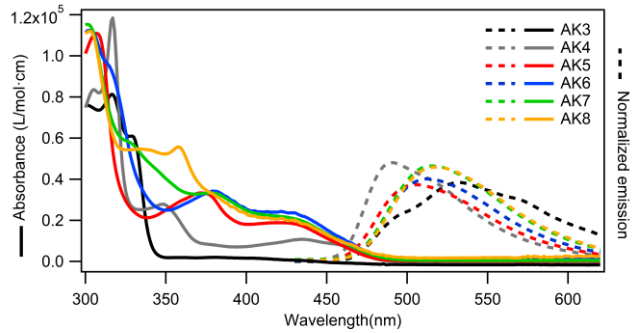

Fig. 4 Compilation of the absorption (—) and emission (...) spectra of the AK3-AK8 (in 1:1 MeCN:C_6H_6) at 22 °C.

The optoelectronic properties of fluorenone was the subject of both experimental and computational studies where the results showed that the observed bands in the UV-vis spectrum correspond to the π to π* transition and n to π* transition is symmetrically forbidden.[59, 60] Therefore, we believe that our AKn systems are showing the same behaviour.

Computational. We performed comparative DFT calculations on our molecules, using the non-standard BLYP35[61] functional which gives reliable results for radical species[62] with double-zeta quality basis set (6-31+G(d,p)) for all optimizations and subsequent studies. It should be noted that some of the calculations are repeated with four other functionals and the results are reported and compared in the ESI; the computational details are provided in the ESI. The calculated HOMO/LUMO energies (Table 1 and Fig. 5) show a decreasing energy gap (E_g = E_{LUMO}–E_{HOMO}) with increasing number of phenylene units for both the AKn and AAn systems. Comparing these values with experimental optical E_g (Table 1)[63] shows acceptable correlation. However, it seems that the DFT overestimates (~2 eV) the E_g values for both AKn and AAn species. The obtained values from the other functionals showed same trend and all of them overestimate the E_g values (Tables S6 and S7, ESI).

We employed the time-dependent density functional theory (TD-DFT) methods to compare the calculated and experimental UV-Vis data. As listed in Table 1, the TD-DFT calculations underestimate the observed λ_{max} by around 40 nm for the AAn species. On the contrary, the TD-DFT data for the AKn compounds show good agreement with the experimental. Analyzing the contributions of the frontier orbitals to the

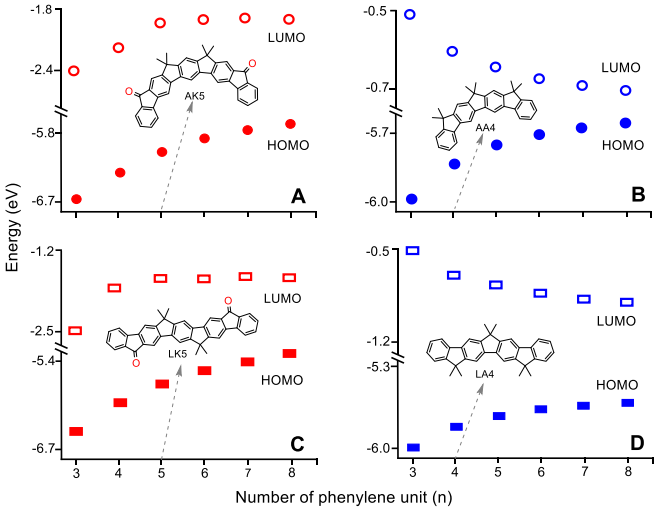

Fig. 5 HOMO (filled) and LUMO (hollow) energies at BLYP35/6-31+G(d,p)+SMD(CH_2Cl_2) level in eV for A) angular keto (AKn), B) angular alkyl (AAn), C) linear keto (LKn) and D) linear alkyl (LAn) species.

observed λ_{max} revealed that the HOMO-to-LUMO transition percentage in the highest observed wavelength (λ_{max}) decreases by increasing the conjugation for both AKn and AAn.[64] This HOMO-to-LUMO transition decrease is more dramatic for AKn species, from 87% to 22%, and much smaller for AAn, from 90% and 71% (Fig. S17-S28, ESI). Therefore, the absorptions of AKn compounds are less sensitive to the E_g in comparison to the AAn compounds and do not show a clear red-shift trend as observed for the AAn series.

In order to understand the charge delocalization of our compounds and comparing them with the Robin-Day classification[65] of charged species, we calculated spin density distributions.[66] Robin and Day classified the polaron (i.e. hole or electron) into three different classes based on the magnitude of the electronic coupling (V_{12}) and structural reorganization energy (λ_{reorg}). In class I, the two redox centers of repeating units are completely localized and act as isolated units with no electronic coupling between them (V_{12} = 0). In class II, the electronic coupling is smaller than the reorganization energy ($\lambda_{reorg} > 2V_{12}$) and the system can show the dynamic hoping of polaron. While the compounds following the class III indicate strong electronic coupling and evenly and static charge delocalization ($2V_{12} > \lambda_{reorg}$).

As illustrated in Fig. 6, the spin density of ≥**AK5** anion radical gravitates to one terminal despite the totally symmetrical LUMOs of neutral species. This means that the injected electron into the system prefers to localize at one terminus. Indeed, comparing the reduction potential of ≥**AK5** with fluorenone supports the DFT results; the E_{red1} of ≥**AK5** and fluorenone is around -1.36 V and -1.37 V, respectively (Table 1 and Fig. S3). In contrast, the **AK3** and **AK4** compounds show charge delocalization. This charge (de)localization change (not following the LUMO pattern) can be attributed to the interplay between the electronic coupling (V_{12}) and structural reorganization energy (λ_{reorg}) from Marcus theory.[67] According to these data, electronic coupling is larger than the

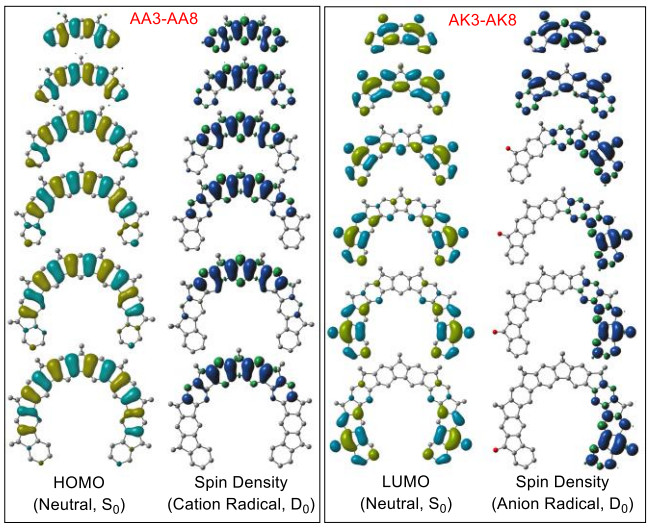

Fig. 6 Isosurface representations (0.02 au) of HOMO and LUMO (for neutral, S_0) and spin density (0.001 au, for anion/cation radical, D_0) for AA3-AA8 (left) and AK3-AK8 (right) molecules at BLYP35/6-31+G(d,p)+SMD(CH_2Cl_2) level.

reorganization energy ($2V_{12} > \lambda_{reorg}$) for **AK3** and **AK4**; they are therefore Robin-Day class III compounds.[65] While, the **AK5-AK8** compounds belong to Robin-Day class II ($2V_{12} < \lambda_{reorg}$)[67] with a dynamic charge hopping mechanism in these acceptor-bridge-acceptor (A-π-A) systems (Fig. S29, ESI).[68-70]

On the other hand, the spin density distribution of the AAn compounds does not show any charge (de)localization switch. The hole is symmetrically distributed (limited to ~4 phenylene units) at the center for all of cation radials, as is typical of conjugated oligomers.[66, 71, 72] The lack of close correspondence between the HOMO and spin density distributions can be attributed to the energetic penalty of λ_{reorg}.[73, 74]

Finally, in order to investigate the effects of the shape of AKn/AAn compounds, we carried out a series of comparative DFT calculations for the linear *para* isomers with both keto (**LK3-LK8**) and alkyl (**LA3-LA8**) bridged termini (Fig. 7A). The results show that the increasing LUMO energy trend is not due to the shape of AKn compounds and can be observed also in the linear keto-bridged species LKn (Fig. 5C). Therefore, we concluded that the presence of electron withdrawing groups (keto) on the termini of the rigid phenylene backbone is responsible for the observed trends in FMO energies and the first reduction potentials.

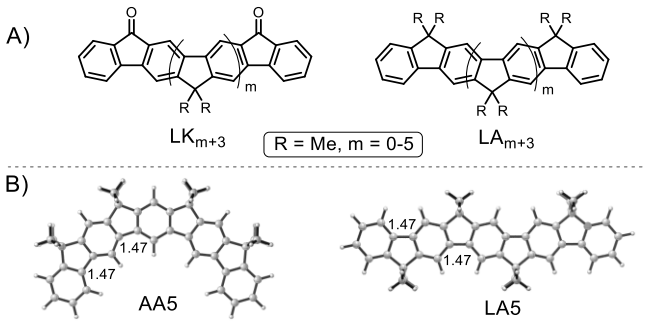

Fig. 7 A) structures of linear LKn and LAn compounds; B) calculated bond lengths [BLYP35/6-31+G(d,p)+ SMD(CH_2Cl_2)] of phenylene linking single bonds for AA5 and LA5 in angstrom.

Moreover, our calculations for oxidation potential of linear compounds (LAn) show that the oxidation energies are systematically lower (5.28 → 4.84 eV, from LA3 to LA8) compared to bent-shaped structures (5.41 → 5.20 eV, from AA3 to AA8). Fig. 7B illustrates the optimized geometries of **AA5** and **LA5**. The C-C bond lengths between phenylene units remain relatively constant for both angular and linear series and are independent of the conjugated length ($bond_{C-C}$=1.47±0.01 Å). This implies that the pi electrons are localized within Clar sextets and there is no bond contraction/elongation.

Conclusion

In summary, we successfully developed the synthesis of a series of π-conjugated angular ladder-type *meta*-phenylenes with two different substituents on their termini, alkyl (AAn) and keto (AKn). Electrochemistry, spectroscopy and DFT methods were used to analyze the electronic properties of all compounds. The results indicated an increase in the first reduction potential (~400 mV) moving from **AK3** to **AK8**. DFT calculations on both synthesized compounds and their linear analogues (**LK3-LK8** and **LA3-LA8**) reveal the progressive increase in LUMO energies and charge localization with the increase of phenylene units in the keto-containing compounds regardless of their shape (linear or angular). This shows us that replacing the alkyl with keto substituents can switch the charge transfer mechanism from the static delocalization (class III) in AAn/LAn to dynamic hopping (class II) in AKn/LKn species. Therefore, we believe that this work shed a new light on the importance of substituent effects on the π-conjugated systems and structure-dependent charge delocalization in oligomers.

Acknowledgements

The authors would like to thank Prof. Scott Reid (Marquette University), Prof. C. Scott Hartley (Miami University) and Prof. Raúl Hernández Sánchez (University of Pittsburgh) for helpful discussions and encouragements. We also thank the NSF (CHE-1508677) and NIH (R01-HL112639-04) for financial support. S.M. thanks the Dietrich School of Arts & Sciences Graduate Fellowship.

Conflict of interest

There are no conflicts to declare.

Abbreviations

AK, angular keto; AA, angular alkyl; LK, linear keto; LA, linear alkyl.

Notes and references

1. G. Povie, Y. Segawa, T. Nishihara, Y. Miyauchi and K. Itami, Synthesis of a carbon nanobelt, *Science.*, 2017, **356**, 172-175
2. Y. Yano, N. Mitoma, H. Ito and K. Itami, A Quest for Structurally Uniform Graphene Nanoribbons: Synthesis, Properties, and Applications, *J. Org. Chem.*, 2020, **85**, 4-33.
3. H. R. Allcock, Rational Design and Synthesis of New Polymeric Material, *Science.*, 1992, **255**, 1106-1112
4. C. Li, M. Liu, N. G. Pschirer, M. Baumgarten and K. Mullen, Polyphenylene-Based Materials for Organic Photovoltaics, *Chem. Rev.*, 2010, **110**, 6817–6855.
5. J. Roncali, P. Leriche and P. Blanchard, Molecular Materials for Organic Photovoltaics: Small is Beautiful, *Adv. Mater.*, 2014, **26**, 3821-3838.
6. A. L. Kanibolotsky, I. F. Perepichka and P. J. Skabara, Star-shaped π-conjugated oligomers and their applications in organic electronics and photonics, *Chem. Soc. Rev.*, 2010, **39**, 2695–2728.
7. Z. Sun, K. Ikemoto, T. M. Fukunaga, T. Koretsune, R. Arita, S. Sato and H. Isobe, Finite phenine nanotubes with periodic vacancy defects, *Science*, 2019, **363**, 151-155.
8. S. Mirzaei, E. Castro and R. H. Sánchez, Tubularenes, *Chem. Sci.*, 2020, **11**, 8089-8094.
9. U. Scherf and K. Müllen, Polyarylenes and poly(arylenevinylenes):A soluble ladder polymer via bridging of functionalized poly(p-phenylene)-precursors *Makromol. Chem. Rapid Commun.*, 1991, **12**, 489-497.
10. M. C. Petty, M. R. Bryce and D. Bloor, *Introduction to Molecular Electronics*, Oxford University Press, New York, 1995.
11. A. C. Grimsdale and K. Mullen, Oligomers and Polymers Based on Bridged Phenylenes as Electronic Materials, *Macromol. Rapid Commun.*, 2007, **28**, 1676-1702.
12. A. C. Grimsdale, K. L. Chan, R. E. Martin, P. G. Jokisz and A. B. Holmes, Synthesis of Light-Emitting Conjugated Polymers for Applications in Electroluminescent Devices, *Chem. Rev.*, 2009, **109**, 897–1091.
13. H.-H. Huang, C. Prabhakar, K.-C. Tang, P.-T. Chou, G.-J. Huang and J.-S. Yang, Ortho-Branched Ladder-Type Oligophenylenes with Two-Dimensionally π-Conjugated Electronic Properties, *J. Am. Chem. Soc.*, 2011, **133**, 8028-8039.
14. K.-T. Wong, L.-C. Chi, S.-C. Huang, Y.-L. Liao, Y.-H. Liu and Y. Wang, Coplanarity in the Backbones of Ladder-type Oligo(p-phenylene) Homologues and Derivatives, *Org. Lett.*, 2006, **8**, 5029-5032.
15. U. Scherf, Ladder-type materials, *J. Mater. Chem.*, 1999, **9**, 1853-1864.
16. M. R. Rao, A. Desmecht and D. F. Perepichka, p-Extended Indenofluorenes, *Chem. Eur. J.*, 2015, **21**, 6193 – 6201.
17. M. M. Hossain, M. V. Ivanov, D. Wang, S. A. Reid and R. Rathore, Spreading Electron Density Thin: Increasing the Chromophore Size in Polyaromatic Wires Decreases Interchromophoric Electronic Coupling, *J. Phys. Chem. C.*, 2018, **122**, 17668-17675.
18. N. F. Phelan and M. Orchin, Cross conjugation, *J. Chem. Educ.*, 1968, **45**, 633-637.
19. C. R. Arroyo, S. Tarkuc, R. Frisenda, J. S. Seldenthuis, C. H. M. Woerde, R. Eelkema, F. C. Grozema and H. S. J. v. d. Zant, Signatures of quantum interference effects on charge transport through a single benzene ring, *Angew. Chem. Int. Ed.*, 2013, **125**, 3234-3237.
20. Y. Li, M. Buerkle, G. Li, A. Rostamian, H. Wang, Z. Wang, D. R. Bowler, T. Miyazaki, L. Xiang, Y. Asai, G. Zhou and N. Tao, Gate controlling of quantum interference and direct observation of anti-resonances in single molecule charge transport, *Nat. Mater.*, 2019, **18**, 357–363.
21. C. M. Guédon, H. Valkenier, T. Markussen, K. S. Thygesen, J. C. Hummelen and S. J. V. D. Molen, observation of quantum interference in molecular charge transport, *Nat. nanotechnol.*, 2012, **7**, 305-309.
22. H. Valkenier, C. M. Guédon, T. Markussen, K. S. Thygesen, S. J. v. d. Molen and J. C. Hummelen, Cross-conjugation and quantum interference: a general correlation?, *Phys. Chem. Chem. Phys.*, 2014, **16**, 653-662.
23. K. G. Pedersen, A. Borges, P. Hedegård, G. C. Solomon and M. Strange, illusory connection between cross-conjugation and quantum interference, *J. Phys. Chem. C.*, 2015, **119**, 26919-26924.
24. X. Li, Z. Tan, X. Huang, J. Bai, J. Liu and W. Hong, Experimental investigation of quantum interference in charge transport through molecular architectures, *J. Mater. Chem. C.*, 2019, **7**, 12790-12808.
25. A. Pogantsch, A. K. Mahler, G. Hayn, R. Saf, F. Stelzer, E. J. W. List, J.-L. Brédas and E. Zojer, Excited-state localization effects in alternating meta- and para-linked poly(phenylene-vinylene)s, *Chem. Phys.*, 2004, **297**, 143-151.
26. U. Scherf and K. Müllen, Polyarylenes and poly(arylenevinylene)s: 8. The first soluble ladder polymer with 1,4-benzoquinone-bismethide subunits, *Polymer*, 1992, **33**, 2443-2446.
27. H. Zhao, L. Cao, S. Huang, C. Ma, Y. Chang, K. Feng, L.-L. Zhao, P. Zhao and X. Yan, Synthesis, Structure, and Photophysical Properties of m-Phenylene-Embedded Cycloparaphenylene Nanorings, *J. Org. Chem.*, 2020, **85**, 6951–6958.
28. G. C. Solomon, D. Q. Andrews, R. H. Goldsmith, T. Hansen, M. R. Wasielewski, R. P. V. Duyne and M. A. Ratner, Quantum interference in acyclic systems: Conductance of crossconjugated molecules, *J. Am. Chem. Soc.*, 2008, **130**, 17301-17308.
29. D. Q. Andrews, G. C. Solomon, R. P. V. Duyne and M. A. Ratner, Single Molecule Electronics: Increasing Dynamic Range and Switching Speed Using Cross-Conjugated Species, *J. Am. Chem. Soc.*, 2008, **130**, 17309-17319.
30. S. Inagi and T. Fuchigami, Electrochemical Post-Functionalization of Conducting Polymers, *Macromol. Rapid Commun.*, 2014, **35**, 854-867.
31. X. Zhaoab and X. Zhan, Electron transporting semiconducting polymers in organic electronics, *Chem. Soc. Rev.*, 2011, **40**, 3728–3743.
32. J. E. Anthony, A. Facchetti, M. Heeney, S. R. Marder and X. W. Zhan, n-Type Organic Semiconductors in Organic Electronics, *Adv. Mater.*, 2010, **22**, 3876-3892.
33. S. Holliday, J. E. Donaghey and I. McCulloch, Advances in Charge Carrier Mobilities of Semiconducting Polymers Used in Organic Transistors, *Chem. Mater.*, 2014, **26**, 647-663.
34. Y. Zhao, Y. Guo and Y. Liu, 25th Anniversary Article: Recent Advances in n-Type and Ambipolar Organic Field-Effect Transistors, *Adv. Mater.*, 2013, **28**, 5372-5391.
35. F. Uckert, Y.-H. Tak, K. Müllen and H. Bässler, 2,7-Poly(9-fluorenone): A Trap-Free Electron-Injection Material with a High Charge Carrier Mobility for Use in Light-Emitting Diodes, *Adv. Mater.*, 2000, **12**, 905–908.
36. T. Lee, C. A. Landis, B. M. Dhar, B. J. Jung, J. Sun, A. Sarjeant, H. J. Lee and H. E. Katz, Synthesis, Structural Characterization, and Unusual Field-Effect Behavior of Organic Transistor Semiconductor Oligomers: Inferiority of Oxadiazole Compared with Other Electron-Withdrawing Subunits *J. Am. Chem. Soc.*, 2009, **131**, 1692–1705.
37. H. Usta, C. Risko, Z. Wang, H. Huang, M. K. Deliomeroglu, A. Zhukhovitskiy, A. Facchetti and T. J. Marks, Design, Synthesis,

and Characterization of Ladder-Type Molecules and Polymers. Air-Stable, Solution-Processable n-Channel and Ambipolar Semiconductors for Thin-Film Transistors via Experiment and Theory, *J. Am. Chem. Soc.*, 2009, **131**, 5586–5608.
38. A. Alanazy, E. Leary, T. Kobatake, S. Sangtarash, M. T. González, H.-W. Jiang, G. R. Bollinger, N. Agräit, H. Sadeghi and I. Grace, Cross-Conjugation Increases the Conductance ofMeta-Connected Fluorenones, *Nanoscale*, 2019, **11**, 13720-13724.
39. H. Meier, Conjugated Oligomers with Terminal Donor–Acceptor Substitution, *Angew. Chem. Int. Ed.*, 2005, **44**, 2482-2506.
40. A. L. Thompson, T.-S. Ahn, K. R. J. Thomas, S. Thayumanavan, T. J. Martínez and C. J. Bardeen, Using Meta Conjugation To Enhance Charge Separation versus Charge Recombination in Phenylacetylene Donor−Bridge−Acceptor Complexes, *J. Am. Chem. Soc.*, 2005, **127**, 16348–16349.
41. D. Wang, M. R. Talipov, M. V. Ivanov and R. Rathore, Energy Gap between the Poly-p-phenylene Bridge and Donor Groups Controls the Hole Delocalization in Donor–Bridge–Donor Wires, *J. Am. Chem. Soc.*, 2016, **138**, 16337-16344.
42. D. E. Ames and A. Opalko, Palladium-catalysed cyclisation of 2-substituted halogenoarenes by dehydrohalogenation, *Tetrahedron.*, 1984, **40**, 1919-1925.
43. Y. Wei, X. Zheng, D. Lin, H. Yuan, Z. Yin, L. Yang, Y. Yu, S. Wang, L.-H. Xie and W. Huang, Superelectrophilic-Initiated C–H Functionalization at the β-Position of Thiophenes: A One-Pot Synthesis of trans-Stereospecific Saddle-Shaped Cyclic Compounds, *J. Org. Chem.*, 2019, **84**, 10701-10709.
44. C. Liu, M. E. Sandoval-Salinas, Y. Hong, T. Y. Gopalakrishna, H. Phan, N. Aratani, T. S. Herng, J. Ding, H. Yamada, D. Kim, D. Casanova and J. Wu, Macrocyclic Polyradicaloids with Unusual Super-ring Structure and Global Aromaticity, *Chem*, 2018, **4**, 1586-1595.
45. M. Rickhaus, M. Jirasek, L. Tejerina, H. Gotfredsen, M. D. Peeks, R. Haver, H.-W. Jiang, T. D. W. Claridge and H. L. Anderson, Global aromaticity at the nanoscale, *Nat. Chem.*, 2020, **12**, 236–241.
46. T. Heinis, S. Chowdhury, S. L. Scott and P. Kebarle, Electron affinities of benzo-, naphtho-, and anthraquinones determined from gas-phase equilibria measurements, *J. Am. Chem. Soc.*, 1988, **110**, 400–407.
47. N. A. Macías-Ruvalcaba, J. P. Telo and D. H. Evans, Studies of the electrochemical reduction of some dinitroaromatics, *J. Elec. Chem.*, 2007, **600**, 294-302.
48. D. H. Evans, One-Electron and Two-Electron Transfers in Electrochemistry and Homogeneous Solution Reactions, *Chem. Rev.*, 2008, **108**, 2113–2144.
49. M. R. Talipov, A. Boddeda, Q. K. Timerghazin and R. Rathore, Key Role of End-Capping Groups in Optoelectronic Properties of Poly-p-phenylene Cation Radicals, *J. Phys. Chem. C.*, 2014, **118**, 21400-21408.
50. C. M. Cardona, W. Li, A. E. Kaifer, D. Stockdale and G. C. Bazan, Electrochemical Considerations for Determining Absolute Frontier Orbital Energy Levels of Conjugated Polymers for Solar Cell Applications, *Adv. Mat.*, 2011, **23**, 2367-2371.
51. D. M. d. Leeuw, M. M. J. Simenon, A. R. Brown and R. E. F. Einerhand, Stability of n-type doped conducting polymers and consequences for polymeric microelectronic devices, *Synth. Met.*, 1997, **87**, 53-59.
52. O. L. Pavlenko, O. P. Dmytrenko, M. P. Kulish, V. A. Sendiuk, N. V. Obernikhina, Y. O. Prostota, O. D. Kachkovsky and L. A. Bulavin, in *Modern Problems of the Physics of Liquid Systems*, eds. L. A. Bulavin and L. Xu, Springer, Cham, 2019, pp. 225-248.
53. S. C. Ciulei and R. R. Tykwinski, Cross-Conjugated Chromophores: Synthesis of iso-Polydiacetylenes with Donor/Acceptor Substitution, *Org. Lett.*, 2000, **2**, 3607–3610.
54. A. Ganguly, J. Zhu and T. L. Kelly, Effect of Cross-Conjugation on Derivatives of Benzoisoindigo, an Isoindigo Analogue with an Extended π-System, *J. Phys. Chem. C.*, 2017, **121**, 9110–9119.
55. G. W. P. v. Pruissen, J. Brebels, K. H. Hendriks, M. M. Wienk and R. A. J. Janssen, Effects of Cross-Conjugation on the Optical Absorption and Frontier Orbital Levels of Donor–Acceptor Polymers, *Macromolecules.*, 2015, **48**, 2435–2443.
56. P. D. Sala, N. Buccheri, A. Sanzone, M. Sassi, P. Neri, C. Talotta, A. Rocco, V. Pinchetti, L. Beverina, S. Brovellib and C. Gaeta, First demonstration of the use of very large Stokes shift cycloparaphenylenes as promising organic luminophores for transparent luminescent solar concentrators, *Chem. Commun.*, 2019, **55**, 3160-3163.
57. F. Vollmer, W. Rettig and E. Birckner, Photochemical mechanisms producing large fluorescence stokes shifts, *J. Fluoresc.*, 1994, **4**, 65–69.
58. W. Ma, W. Li, M. Cao, R. Liu, X. Zhao and X. Gong, Large Stokes-shift AIE fluorescent materials for high-performance luminescent solar concentrators, *Org. Electron.*, 2019, **73**, Pages 226-230.
59. A. Devaux, C. Minkowski and G. Calzaferri, Electronic and Vibrational Properties of Fluorenone in the Channels of Zeolite L, *Chem. Eur. J.*, 2004, **10**, 2391-2408.
60. O. K. Bazyl', V. I. Danilova and R. M. Fofonova, Nature of the long-wave UV absorption band of fluorenone, *J. Appl. Spectrosc.*, 1976, **24**, 665–667.
61. M. Renz, K. Theilacker, C. Lambert and M. Kaupp, A Reliable Quantum-Chemical Protocol for the Characterization of Organic Mixed-Valence Compounds, *J. Am. Chem. Soc.*, 2009, **131**, 16292-16302
62. M. Renz, M. Kess, M. Diedenhofen, A. Klamt and M. Kaupp, Reliable Quantum Chemical Prediction of the Localized/Delocalized Character of Organic Mixed-Valence Radical Anions. From Continuum Solvent Models to Direct-COSMO-RS, *J. Chem. Theory Comput.*, 2012, **8**, 4189-4203.
63. J. C. Costa, R. J. Taveira, C. F. Lima, A. Mendes and L. M. Santos, Optical band gaps of organic semiconductor materials, *Opt. Mater.*, 2016, **58**, 51–60.
64. H. Meier, J. Gerold, H. Kolshorn and B. Muhling, Extension of Conjugation Leading to Bathochromic or Hypsochromic Effects in OPV Series, *Chem. Eur. J.*, 2004, **10**, 360-370.
65. M. B. Robin and P. Day, Mixed Valence Chemistry-A Survey and Classification, *Adv. Inorg. Chem. Radiochem.*, 1968, **10**, 247-422.
66. M. V. Ivanov, S. A. Reid and R. Rathore, Game of Frontier Orbitals: A View on the Rational Design of Novel Charge-Transfer Materials, *J. Phys. Chem. Lett.*, 2018, **9**, 3978-3986.
67. A. Heckmann and C. Lambert, Organic Mixed-Valence Compounds: A Playground for Electrons and Holes, *Angew. Chem. Int. Ed.*, 2012, **51**, 326-392.
68. M. V. Ivanov, V. J. Chebny, M. R. Talipov and R. Rathore, Poly-p-hydroquinone Ethers: Isoenergetic Molecular Wires with Length-Invariant Oxidation Potentials and Cation Radical Excitation Energies, *J. Am. Chem. Soc.*, 2017, **139**, 4334-4337.
69. M. R. Talipov, T. S. Navale, M. M. Hossain, R. Shukla, M. V. Ivanov and R. Rathore, Dihedral-Angle-Controlled Crossover from Static Hole Delocalization to Dynamic Hopping in Biaryl Cation Radicals, *Angew. Chem. Int. Ed.*, 2017, **56**, 266-269.
70. P. M. Burrezo, N.-T. Lin, K. Nakabayashi, S. Ohkoshi, E. M. Calzado, P. G. Boj, M. A. Díaz-García, C. Franco, C. Rovira, J.

Veciana, M. Moos, C. Lambert, J. T. L. p. Navarrete, H. Tsuji, E. Nakamura and J. Casado, Bis(aminoaryl) Carbon-Bridged Oligo-(phenylenevinylene)s Expand the Limits of Electronic Couplings, *Angew. Chem., Int. Ed.* , 2017, **56**, 2898–2902.

71. R. E. Larsen, Simple Extrapolation Method To Predict the Electronic Structure of Conjugated Polymers from Calculations on Oligomers, *J. Phys. Chem. C.* , 2016, **120**, 9650-9660.

72. M. V. Ivanov, R. Shukla, S. V. Lindeman, D. Wang and R. Rathore, Pyrene-Like HOMO Governs Polaron Delocalization in Model Graphitic Strips: A Combined Experimental and Computational Analysis, *J. Phys. Chem. C.*, 2018, **122**, 24527-24534.

73. M. V. Ivanov, M. R. Talipov, A. Boddeda, S. H. Abdelwahed and R. Rathore, Hückel Theory + Reorganization Energy = Marcus–Hush Theory: Breakdown of the 1/n Trend in π-Conjugated Poly-p-phenylene Cation Radicals Is Explained, *J. Phys. Chem. C.*, 2017, **121**, 1552-1561.

74. L. Zaikowski, P. Kaur, C. Gelfond, E. Selvaggio, S. Asaoka, Q. Wu, H.-C. Chen, N. Takeda, A. R. Cook, A. Yang, J. Rosanelli and J. R. Miller, Polarons, Bipolarons, and Side-By-Side Polarons in Reduction of Oligofluorenes, *J. Am. Chem. Soc.*, 2012, **134**, 10852-10863.